Supporting Information

Bontognali et al. 10.1073/pnas.1207491109

SI Text

SI Discussion. NanoSIMS $\delta^{34}S$ analysis of the extracted kerogen yielded data that overlap with but are, on average, more negative than values obtained by in situ measurements performed directly on the stromatolite thin sections (Fig. 3). Given the challenges associated with the statistics of small numbers, it is not simple to assess whether the characteristics of these distributions are meaningfully different, or would instead converge given more observations of other regions of the stromatolite. If the distributions are indeed real, several factors might explain this difference:

1. The portion of stromatolite sample used for extracting kerogen via HF/HCl dissolution of the rock matrix may not be representative of the regions analyzed in situ.

2. Some S-bearing molecules (e.g., disulfides and polysulfides) may be lost during the HF/HCl demineralization procedure. However, this process is not expected to cause large isotopic fractionation of the remaining organic sulfur (1).

3. A fraction of the signal for in situ measurements may come from elemental sulfur that formed by recent oxidation with atmospheric oxygen. Such elemental sulfur would be lost during the HF/HCl demineralization procedure used for isolation of kerogen. Few studies have determined the effect of oxidation processes on the isotopic composition of organic sulfur. However, existing data indicate that only limited isotopic fractionation occurs during oxidation, leaving the $\delta^{34}S$ values of the remaining sulfur basically unaltered (2). Moreover, abiotic oxidation processes typically favor ^{32}S over ^{34}S. Thus, measurements of extracted kerogen, which do not include the oxidized S, should yield, on average, more positive $\delta^{34}S$ values relative to the in situ measurements. Our data indicate the opposite trend.

4. The in situ measurements performed on cherts may be subtly influenced by a matrix effect. It is difficult to categorically exclude this hypothesis; however, a matrix effect could be expected to preferentially increase counts of the lighter isotope (3). Comparison of data for kerogens and in situ analyses indicate the opposite trend. Also, no correlation exists between $\delta^{34}S$ and Si/C ratios, nor between $\delta^{34}S$ and O/C ratios (where Si/C and O/C are proxies for the amount of chert matrix relative to the amount of organic material), suggesting the absence of a large matrix effect.

5. Mechanical mixing during the extraction process may homogenize the organic material. This could explain the slightly smaller range of $\delta^{34}S$ values in the extracted kerogen and—in conjunction with point 1—potentially the difference in average values.

6. A fraction of the signal from in situ measurements may derive from carbonate minerals containing traces of sulfate. We do not favor this hypothesis because explicit measurements of coexisting carbonate minerals in the thin section yielded a S ion count two orders of magnitude lower than those from organic regions. This comparison also excludes a possible source of background contamination.

7. NanoSIMS measurements are feasible only on organic particles with minimum dimensions of 3 × 3 μm. Smaller particles, which represent an important fraction of the bulk extracted organic material but were not analyzed in situ, could have lower average $\delta^{34}S$ values.

The precise influence of these factors in the resulting differences between the $\delta^{34}S$ distributions remains undetermined. However, the results from both in situ measurements and extracted kerogen, even when considered separately, point to the same conclusion: The process of organic matter sulfurization in pore waters was influenced by sulfur-metabolizing microbes.

SI Methods. *Sample preparation for in situ measurements.* Stromatolite samples investigated in this study were collected from an outcrop located on southern Anchor Ridge in the northern Pilbara Craton, Western Australia. The exact location of the outcrop, a detailed petrographic description of the sample, and its stratigraphic position are described in detail by ref. 4. Ultrapolished thin sections for NanoSIMS analysis were produced from the sample pictured in Allwood et al.'s figure 1 (4). Thin sections were coated with 30 nm of Au to provide optimal electrical conductivity. To avoid contamination, immersion oil was never used during preliminary investigation by optical microscopy and samples were mounted to the glass without complete impregnation into Epoxy. Samples were cleaned by ultrasonication in high-purity ethanol prior to application of the gold coating.

Extraction of bulk organic matter by HF/HCl demineralization. Samples were first crushed and then demineralized by acidification in HCl followed by HF. About 30 g of sample was placed into aqua regia and solvent-cleaned Teflon tubes (approximately 10 g per tube). Acids were then added to the samples and allowed to react as follows: 6N DCM-extracted HCl for 24–48 h (to remove carbonates) and 48% HF for at least 72 h (to dissolve silicates). In this latter step, we used a modification of the procedure described in ref. 5 whereby we added solid boric acid to the HF digestion to inhibit formation of fluorides. The samples were then washed several times in DCM-extracted HCl followed by DCM-extracted water. The resulting powders were re-extracted and dried. The resulting kerogen had a bulk carbon isotopic composition of $-27.8‰$ VPDB.

For NanoSIMS analysis, the extracted organic matter was mounted on a steel holder by pressing the powder into a layer of indium metal. Due to the very limited amount of kerogen, it was not possible to analyze the extracted organic material by elemental analyzer–isotope ratio mass spectrometry (EA-IRMS).

Kerogen standards. In addition to the organic matter extracted from the stromatolite sample, four kerogens were used as standards for this study, including: type III-S (Miocene Monterey Formation) (6), type IIS (Cretaceous Ghareb limestone from Jordan) (7), type III (Paleocene lignite from Calvert Bluff Formation of the Wilcox Group in Texas) (7), and protokerogen from the Santa Barbara Basin. The method used for isolating the kerogens is described in ref. 7.

The bulk $\delta^{34}S$ composition of the kerogens was determined at the University of California, Riverside, CA using standard elemental analyzer-isotopic ratio mass spectrometer (EA-IRMS) method (8, 9).

For IMS 7f and NanoSIMS analysis, the kerogen standards were mounted on steel holders by pressing the powders into a layer of indium.

IMS 7f-GEO analysis. The extracted kerogens were investigated with a Cameca 7f-GEO magnetic sector secondary ion mass spectrometer at the Center for Microanalysis of the California Institute of Technology, Pasadena, CA. This ion probe provides lower spatial resolution but higher measurement precision when compared to NanoSIMS. Analytical conditions for session 1 (Table S2) were as follows: presputtering, 10 × 10 μm; data collection,

10 × 10 μm; all masses were measured with Faraday cup (FC) detectors; beam current was approximately 6.5 nA. Analytical conditions for sessions 2 and 3 (Table S2) were as follows: presputtering, 10 × 10 μm; data collection, focused beam; all masses were measured with electron multiplier (EM) detectors, beam current was approximately 0.2 nA. Analytical conditions for session 4 (Table S3) were as follows: presputtering, 50 × 50 μm; data collection, 50 × 50 μm; ^{32}S was measured with FC detector, ^{33}S was measured with EM detector, and ^{34}S was measured with EM detector; beam current was approximately 3 nA. Analytical conditions for session 5 (Table S3) were as follows: presputtering, 5 × 5 μm; data collection, 5 × 5 μm; ^{32}S was measured with FC detector, ^{33}S with EM detector, and ^{34}S with EM detector; beam current was approximately 0.2 nA. Instrument mass fractionation during each session was corrected by calibration to the kerogen standard from the Monterey Formation. Δ^{33}S measurements are based on the assumption that organic sulfur in kerogens younger than 2.4 billion years (Ga) (the time when anomalous Δ^{33}S disappear from sedimentary sulfide likely due to the oxygenation of the atmosphere) has a Δ^{33}S = 0 (10). This assumption was not independently tested by measuring Δ^{33}S of the kerogens with a bulk method.

NanoSIMS analysis. Isotope ratio measurements were performed using the Cameca NanoSIMS 50L at the Center for Microanalysis of the California Institute of Technology, Pasadena, CA. Analyses of organic material were carried out by rastering an approximately 20 nA Cs$^+$ ion beam across presputtered 3 × 3 μm regions of the samples. The secondary ions species ^{12}C$^-$, ^{16}O$^-$, ^{28}Si$^-$, ^{32}S$^-$, and ^{34}S$^-$ were recorded simultaneously by electron multipliers. The regions of interest were located using the NanoSIMS charge coupled device camera and real-time ^{12}C and ^{32}S ion imaging. Data were collected in 16 analytical sessions over a period of one year. The results of each session are presented in Table S4 and Fig. S4 in the original sequence of the measurements. All analyses of the samples were interspersed with multi-

ple measurements of a standard. Instrument mass fractionation during each session was corrected by calibration to the kerogen standard from the Monterey Formation. No systematic drift in the recorded ^{34}S/^{32}S ion-current ratios due to detector ageing was observed when comparing measurements of the standards at the beginning and end of each session. Thus, no drift correction has been applied. Incomplete coverage corrections were not necessary because the analyses were performed exclusively on regions in which organic material filled the 3 × 3 μm raster area. Raw ^{34}S/^{32}S ratios were corrected for electron multiplier deadtime, and corrected for quasi-simultaneous arrivals (QSA) using the relationship $R_{measured} = R_{true} \cdot (1 + \beta \cdot K)$; with $\beta = 0.5$ and $K = {}^{32}S^-/Cs^+$ (11, 12). Because questions persist concerning the general validity of this formula (11, 12), we recalculated our data both without QSA correction and by applying the QSA correction with $\beta = 0.69$ [i.e., the value obtained experimentally through the measurement of sulfide minerals (11)]. By using the QSA correction with $\beta = 0.5$, the δ^{34}S values measured from the stromatolites (session 1 to session 13 in Table S4) range from 16.6‰ to 40.6‰. If we do not apply the QSA correction, δ^{34}S range from 19.9‰ to 36.6‰, and, on average, they are 3.4‰ more negative than the values corrected with $\beta = 0.5$. By applying the QSA correction with $\beta = 0.69$, δ^{34}S values range from 15.4‰ to 42.2‰ and are, on average, 1.3‰ more positive than the values corrected with $\beta = 0.5$. Such differences are small relative to the total range of measured δ^{34}S values (>56‰ in all three cases) and so do not influence our interpretation of the data. In Table S4, data are reported both with and without QSA correction. Measurements performed on the four kerogens of known isotopic composition indicate that NanoSIMS data match slightly better those obtained with IMS 7f-GEO if no QSA correction is applied. Thus, Fig. 1 and Fig. 3 were based on data without QSA correction. No correlation between δ^{34}S and Si/C, δ^{34}S and O/C, or δ^{34}S and ^{32}S count rate were observed during any of the in situ measurements. Such correlations could be diagnostic of analytical artifacts due to the presence of the mineral matrix.

1. Amrani A, Lewan MD, Aizenshtat Z (2005) Stable sulfur isotope partitioning during simulated petroleum formation as determined by hydrous pyrolysis of Ghareb Limestone, Israel. *Geochim Cosmochim Acta* 69:5317–5331.
2. Fry B, Ruf W, Gest H, Hayes JM (1988) Sulfur isotope effects associated with oxidation of sulfide by O$_2$ in aqueous solution. *Isot Geosci* 73:205–210.
3. Riciputi LR, Paterson BA, Ripperdan RL (1998) Measurement of light stable isotope ratios by SIMS: Matrix effects for oxygen, carbon, and sulfur isotopes in minerals. *Int J Mass Spectrom* 178:81–112.
4. Allwood AC, et al. (2006) Controls on development and diversity of Early Archean stromatolites. *Proc Natl Acad Sci USA* 106:9548–9555.
5. Robl TL, Davis BH (1993) Comparison of the HF-HCl and HF-BF 3 maceration techniques and the chemistry of resultant organic concentrates. *Org Geochem* 20:249–255.
6. Schimmelmann A, Lawrence M, Michael E (2001) Stable sotope rations of organic H, C, and N in the Miocene Monterey Formation, Califronia. *The Monterey Formation; From Rocks to Molecules*, eds Isaac CM, Rullkoetter J (Columbia Univ Press, New York), pp 86–106.

7. Schimmelmann A, Lewan MD, Wintsch RP (1999) D/H isotope ratios of kerogen, bitumen, oil, and water in hydrous pyrolysis of source rocks containing kerogen types I, II, IIS, and III. *Geochim Cosmochim Acta* 63:3751–3766.
8. Giesemann A, Jaeger HJ, Norman AL, Krouse HR, Brand WA (1994) Online sulfur-isotope determination using an elemental analyzer coupled to a mass spectrometer. *Anal Chem* 66:2816–2819.
9. Studley SA, et al. (2002) Analysis of sulfides in whole rock matrices by elemental analyzer-continuous flow isotope ratio mass spectrometry. *Chem Geol* 192:141–148.
10. Johnston DT (2011) Multiple sulfur isotopes and the evolution of Earth's surface sulfur cycle. *Earth Sci Rev* 106:161–183.
11. Fike DA, Gammon CL, Ziebis W, Orphan VJ (2008) Micron-scale mapping of sulfur cycling across the oxycline of a cyanobacterial mat: a paired nanoSIMS and CARD-FISH approach. *ISME J* 2:749–759.
12. Slodzian G, Hillion F, Stadermann FJ, Zinner E (2004) QSA influences on isotopic ratio measurements. *Appl Surf Sci* 231–232:874–877.
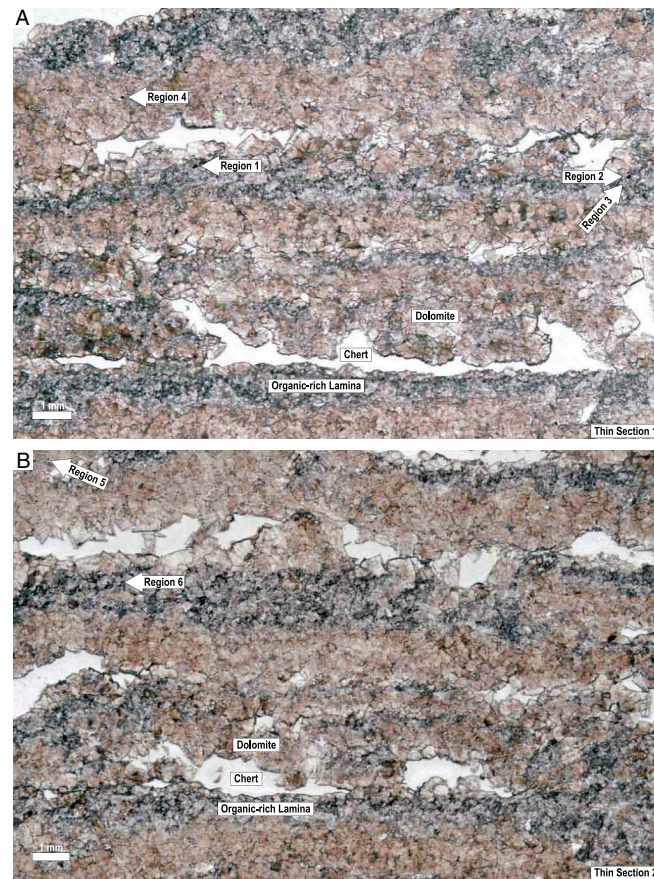
Fig. S1. Thin sections of the stromatolite sampled for nanoSIMS analysis. (*A* and *B*) Images were produced using a slide scanner. Arrows indicate the six regions (Fig. 2) where in situ measurements were performed.
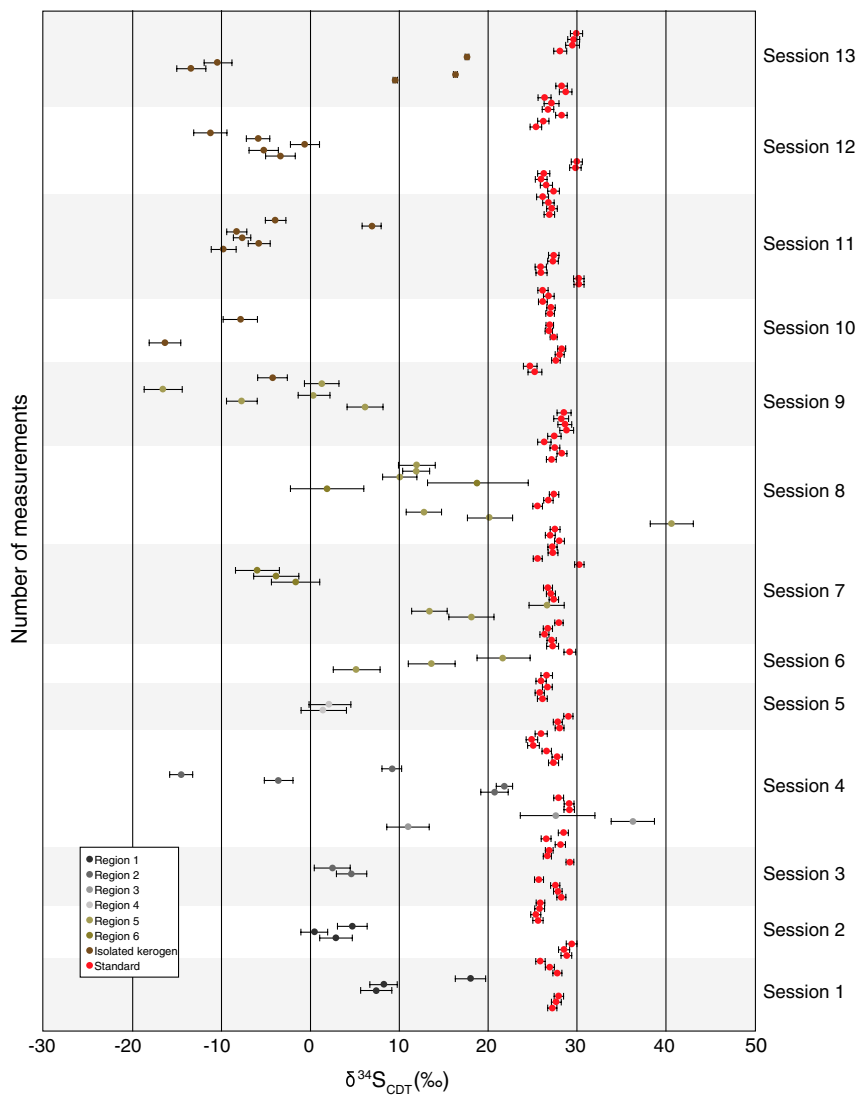
Fig. S2. Sulfur isotope data plotted in analytical sequence. Instrument mass fractionation during each session was corrected via linear regression relative to the Monterey kerogen (red dots), which has a bulk $\delta^{34}S$ value of 27.2‰. Error bars indicate internal error (1σ).
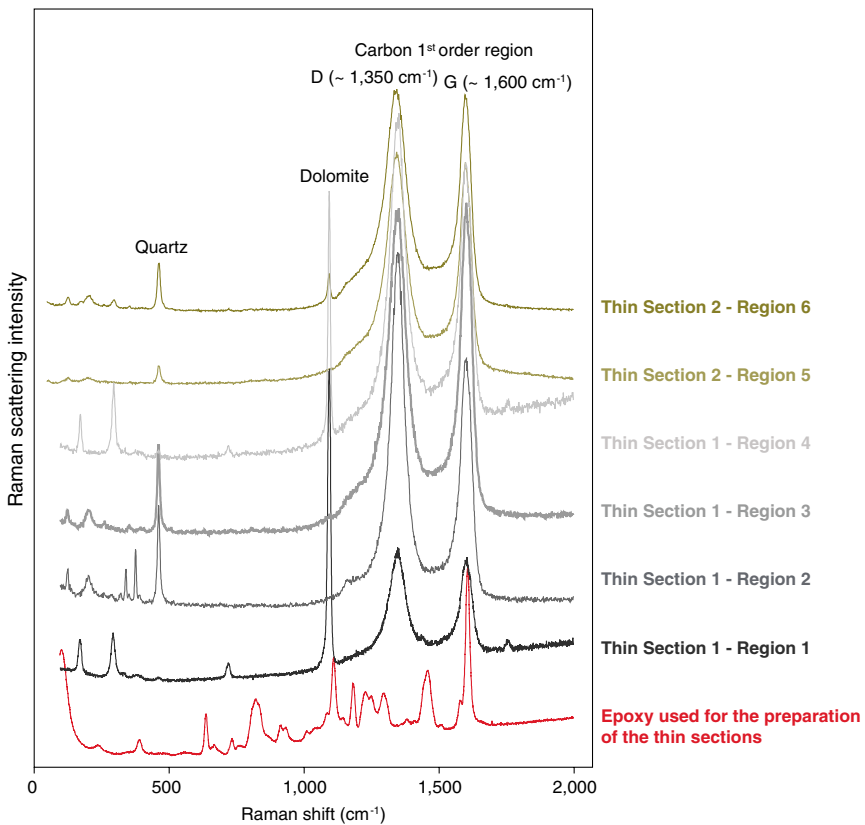
Fig. S3. Representative Raman spectra of the organic-rich regions analyzed by NanoSIMS. Main peaks correspond to quartz, dolomite, and disordered carbonaceous material (G and D bands in the carbon first-order region). Spectra were acquired using a Renishaw MicroRaman Spectrometer with argon ion laser (514.5 nm).
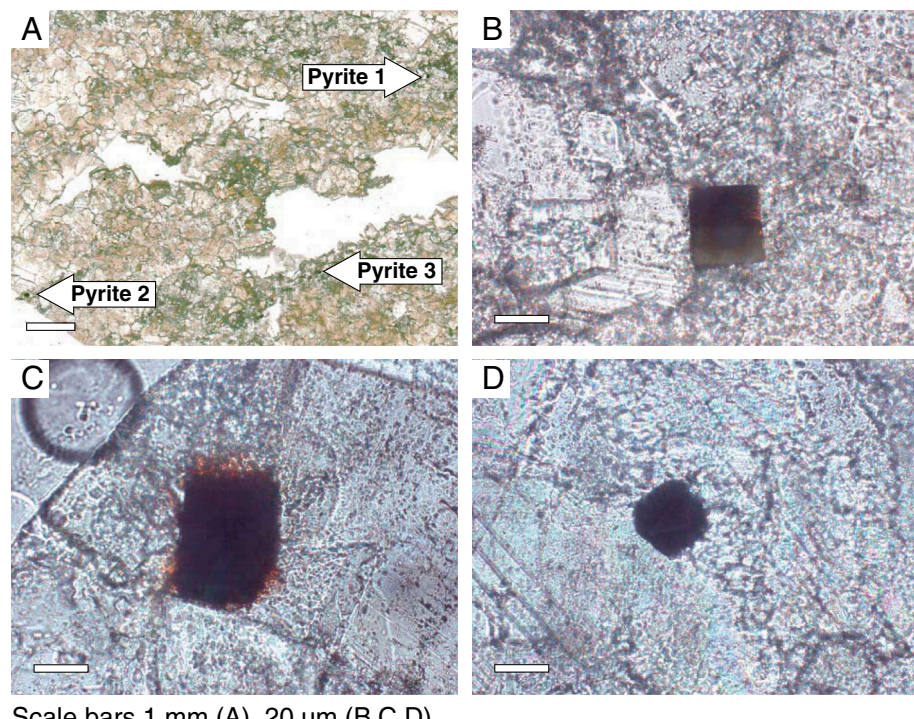
Scale bars 1 mm (A), 20 μm (B,C,D)

Fig. S4. Pyrite crystals present within the investigated stromatolite. (*A*) Overview of the thin section produced using a slide scanner. Arrows indicate the location of the pyrite crystals within the stromatolite. Scale bar, 1 mm. (*B–E*) Transmitted light photomicrographs showing the pyrite crystals that were analyzed by ion probe. Scale bars, 20 μm.

Table S1. Data from IRMS analyses

Sample*	Amount, mg	Wt. % S	Wt. % C[†]	Wt. % S/C	δ^{34}S
MON	0.400	14.9	49.9	0.30	26.6
MON	0.399	15.2	49.9	0.30	27.4
MON	0.400	15.0	49.9	0.30	27.5
MON	0.402	14.8	49.9	0.30	27.3
MON	0.406	15.4	49.9	0.31	27.4
GHA	0.379	13.5	64.8	0.21	13.2
GHA	0.423	13.2	64.8	0.20	10.7
SBB	0.410	8.4	44.8	0.19	-22.9
SBB	0.398	8.7	44.8	0.19	-23.6
WIL	5.106	6.8	68.2	0.10	7.6
WIL	4.999	3.8	68.2	0.06	8.1

*MON, kerogen isolated from Monterey Formation; GHA, kerogen from Ghareb Limestone; SBB, protokerogen from Santa Barbara Basin sediments; WIL, kerogen from the Wilcox group.
[†]Wt % C values were measured during a separate session.

Table S2. Data from IMS-7f analyses

| Session	Sample*	^{32}S cps[†]	raw δ^{34}S[‡]	δ^{34}S[§]	σ_{int}[¶]	Σ_{IF}[‖]	^{32}S/^{12}C
1	Standard	150721193	4.9	26.9	0.4	1.4	0.91
1	Standard	109211507	4.2	26.2	0.3	1.4	0.66
1	Standard	162223253	4.7	26.7	0.3	1.4	0.89
1	Standard	127255113	5.1	27.1	0.3	1.4	0.75
1	Standard	104042480	3.5	25.5	0.2	1.4	0.69
1	Standard	110730547	4.5	26.5	0.2	1.4	0.71
1	Standard	119543840	4.8	26.8	0.3	1.4	0.76
1	Standard	101266626	5.9	27.9	0.5	1.4	0.70
1	Standard	95285724	5.5	27.5	0.4	1.4	0.67
1	Standard	114310710	6.6	28.6	0.4	1.4	0.75
1	GHA	75520832	−12.7	9.3	0.3	1.4	0.76
1	GHA	65847908	−9.7	12.3	0.5	1.4	0.75
1	GHA	76810846	−11.1	10.9	0.3	1.4	0.73
1	GHA	73751044	−9.3	12.7	0.3	1.4	0.74
1	GHA	128501474	−10.5	11.5	0.5	1.4	0.80
1	GHA	136182490	−11.0	11.0	0.2	1.4	0.77
1	GHA	121598090	−10.2	11.8	0.3	1.4	0.76
1	GHA	124813733	−11.2	10.8	0.2	1.4	0.76
1	GHA	118557303	−11.8	10.2	0.3	1.4	0.73
1	GHA	130004027	−12.2	9.8	0.2	1.4	0.77
1	SBB	249589177	−54.6	−32.6	0.4	1.4	1.69
1	SBB	124701017	−45.6	−23.6	0.3	1.4	0.77
1	SBB	103417915	−45.0	−23.0	0.5	1.4	0.61
1	SBB	171557810	−50.2	−28.2	0.3	1.4	1.05
1	SBB	147372343	−40.3	−18.3	0.5	1.4	0.92
1	SBB	136940430	−45.2	−23.2	0.5	1.4	0.96
1	SBB	82123894	−42.4	−20.4	0.3	1.4	0.59
1	SBB	117404464	−52.9	−30.9	0.4	1.4	0.81
1	SBB	108221298	−42.9	−20.9	0.3	1.4	0.88
1	SBB	178369817	−45.4	−23.4	0.4	1.4	1.25
1	SBB	104947027	−45.1	−23.1	0.8	1.4	0.68
1	SBB	99735236	−43.6	−21.6	0.5	1.4	0.65
1	Standard	13497652	6.7	28.7	0.7	1.4	0.58
1	Standard	13408442	5.3	27.3	0.7	1.4	0.62
1	Standard	14926185	6.5	28.5	0.8	1.4	0.58
1	Standard	16176984	6.7	28.7	0.8	1.4	0.55
1	Standard	33783324	7.2	29.2	0.5	1.4	0.72
1	GHA	133126120	−9.8	12.2	0.2	1.4	0.80
1	GHA	127247897	−10.8	11.2	0.2	1.4	0.76
1	GHA	128790780	−10.7	11.3	0.2	1.4	0.80
1	GHA	117583293	−13.3	8.7	0.2	1.4	0.76
1	GHA	122174910	−9.8	12.2	0.2	1.4	0.75
1	WIL	27783114	−16.2	5.8	0.3	1.4	0.051
1	WIL	30449841	−18.0	4.0	0.4	1.4	0.048
1	WIL	28249800	−17.3	4.7	0.2	1.4	0.048
1	WIL	33244760	−19.1	2.9	1.4	1.4	0.048
1	WIL	24751366	−17.1	4.9	0.6	1.4	0.050
1	WIL	30851787	−19.6	2.4	0.3	1.4	0.049
1	WIL	26692232	−21.4	0.6	2.1	1.4	0.047
1	WIL	30860679	−22.2	−0.2	0.3	1.4	0.054
1	WIL	29419364	−16.4	5.6	0.6	1.4	0.042

Session	Sample*	^{32}S cps[†]	raw δ^{34}S[‡]	δ^{34}S[§]	σ_{int}[¶]	Σ_{IF}[‖]	^{32}S/^{12}C
1	WIL	28256023	−18.9	3.1	0.4	1.4	0.045
1	Standard	365861530	4.8	26.8	0.2	1.4	0.753
1	Standard	335844225	5.4	27.4	0.2	1.4	0.807
1	Standard	154928815	6.2	28.2	0.3	1.4	0.898
1	Standard	361880440	1.5	23.5	0.7	1.4	1.034
1	Standard	340484225	3.6	25.6	0.3	1.4	0.828
1	GHA	278830395	−11.3	10.7	0.3	1.4	0.862
1	GHA	275497295	−11.4	10.6	0.5	1.4	0.830
2	Standard	245489	8.8	28.2	1.0	1.9	0.66
2	Standard	232561	7.9	27.3	0.8	1.9	0.62
2	Standard	229092	8.3	27.6	0.9	1.9	0.67
2	Standard	242065	4.9	24.2	1.0	1.9	0.77
2	Standard	301627	7.7	27.0	0.9	1.9	0.85
2	Standard	286679	10.6	30.0	1.0	1.9	0.96
2	Standard	223664	5.2	24.5	1.2	1.9	0.96
2	Standard	201721	5.4	24.7	1.0	1.9	1.10
2	Standard	304660	7.3	26.6	1.0	1.9	0.72
2	Standard	283670	10.2	29.6	0.9	1.9	0.69
2	OM	143391	−32.4	−13.1	1.7	1.9	0.36
2	OM	139411	−32.1	−12.8	1.3	1.9	0.27
2	OM	151299	−34.0	−14.6	1.2	1.9	0.31
2	OM	157973	−32.2	−12.9	2.1	1.9	0.25
2	OM	164323	−34.3	−14.9	1.5	1.9	0.32
2	Standard	374591	6.5	25.8	0.9	1.9	0.69
2	Standard	386446	8.5	27.9	1.0	1.9	0.67
2	Standard	433415	10.9	30.3	0.7	1.9	0.72
2	Standard	416575	7.9	27.2	0.9	1.9	0.74
3	Standard	272949	9.1	28.2	0.9	1.9	0.81
3	Standard	309715	7.7	26.8	1.1	1.9	1.02
3	Standard	245489	8.8	27.9	1.0	1.9	0.66
3	Standard	232561	7.9	27.0	0.8	1.9	0.62
3	Standard	229092	8.3	27.4	0.9	1.9	0.67
3	Standard	242065	4.9	24.0	1.0	1.9	0.77
3	Standard	301627	7.7	26.8	0.9	1.9	0.85
3	Standard	286679	10.6	29.7	1.0	1.9	0.96
3	Standard	223664	5.2	24.3	1.2	1.9	0.96
3	Standard	201721	5.4	24.5	1.0	1.9	1.10
3	Standard	304660	7.3	26.4	1.0	1.9	0.72
3	Standard	283670	10.2	29.3	0.9	1.9	0.69
3	OM	143391	−32.4	−13.3	1.7	1.9	0.36
3	OM	139411	−32.1	−13.0	1.3	1.9	0.27
3	OM	151299	−34.0	−14.9	1.2	1.9	0.31
3	OM	157973	−32.2	−13.1	2.1	1.9	0.25
3	OM	164323	−34.3	−15.2	1.5	1.9	0.32
3	Standard	394400	10.4	29.5	1.1	1.9	1.00
3	Standard	374591	6.5	25.6	0.9	1.9	0.69
3	Standard	386446	8.5	27.6	1.0	1.9	0.67
3	Standard	433415	10.9	30.0	0.7	1.9	0.72
3	Standard	416575	7.9	27.0	0.9	1.9	0.74
3	OM	124366	−26.8	−7.7	2.0	1.9	0.21
3	OM	127985	−21.9	−2.8	2.1	1.9	0.18
3	OM	136396	−27.3	−8.2	1.9	1.9	0.20
3	OM	77752	−22.2	−3.1	2.3	1.9	0.27
3	OM	56852	−30.7	−11.6	2.7	1.9	0.20
3	OM	152961	−26.7	−7.6	1.7	1.9	0.19
3	OM	112715	−33.5	−14.4	2.1	1.9	0.21
3	OM	113631	−22.9	−3.8	1.4	1.9	0.19

*Standard, kerogen isolated from Monterey Formation; SBB, protokerogen from recent Santa Barbara Basin sediments; GHA, kerogen from Ghareb Limestone; WIL, kerogen from the Wilcox group; OM, kerogen extracted from Strelley Pool stromatolite.

[†]^{32}S ion current expressed in counts per second.

[‡]Raw sulfur isotope composition of kerogen (i.e., noncorrected for instrumental mass fractionation) expressed in ‰ relative to the V-CDT standard.

[§]Sulfur isotope composition of kerogen corrected for instrumental mass fractionation and expressed in ‰ relative to the V-CDT standard.

[¶]Internal error (1σ).

[‖]Standard deviation (1σ) for the linear regression used to correct for the instrumental mass fractionation during each session.

Table S3. Data from IMS-7f analyses including ^{33}S

Session	Sample*	^{32}S cps†	raw $\delta^{34}S$‡	$\delta^{34}S$§	σ_{int}¶	Σ_{IF}‖	raw $\Delta^{33}S$	σ_{int}	raw $\Delta^{33}S$**	$\Delta^{33}S$	Σ_{IF}††
4	OM	5915171	6.9	−12.7	0.3	2.8	14.7	0.3	11.1	0.6	0.5
4	OM	6060225	9.4	−10.2	0.4	2.8	17.0	0.4	12.1	1.5	0.5
4	OM	6725554	6.8	−12.8	0.3	2.8	16.2	0.5	12.6	2.1	0.5
4	OM	5749545	8.1	−11.5	0.3	2.8	16.0	0.4	11.8	1.3	0.5
4	MON	17087775	49.6	30.0	0.2	2.8	36.1	0.2	10.4	−0.2	0.5
4	MON	17791051	49.5	29.9	0.2	2.8	36.2	0.2	10.5	0.0	0.5
4	MON	17990420	48.4	28.8	0.1	2.8	35.7	0.2	10.6	0.1	0.5
4	MON	17789843	48.0	28.4	0.2	2.8	35.3	0.2	10.4	−0.1	0.5
4	GHA	2953099	37.1	17.5	0.3	2.8	30.9	0.3	11.7	1.1	0.5
4	GHA	4779879	36.7	17.1	0.3	2.8	29.7	0.3	10.7	0.1	0.5
4	GHA	4030874	34.1	14.5	0.2	2.8	28.2	0.4	10.5	−0.1	0.5
4	GHA	6653332	37.8	18.2	0.3	2.8	31.0	0.2	11.4	0.8	0.5
4	WIL	7415625	25.9	6.3	0.2	2.8	24.1	0.2	10.7	0.2	0.5
4	WIL	6469002	17.4	−2.2	0.3	2.8	19.4	0.3	10.4	−0.2	0.5
4	WIL	7599388	23.7	4.1	0.2	2.8	22.4	0.3	10.1	−0.4	0.5
4	WIL	7437088	22.5	2.9	0.3	2.8	22.3	0.3	10.7	0.1	0.5
4	OM	5633382	4.8	−14.8	0.4	2.8	13.5	0.5	11.0	0.5	0.5
4	OM	5695818	5.9	−13.7	0.3	2.8	13.4	0.4	10.4	−0.2	0.5
4	OM	5475231	6.5	−13.1	0.3	2.8	14.5	0.4	11.1	0.6	0.5
4	OM	7436494	3.6	−16.0	0.2	2.8	14.1	0.3	12.2	1.6	0.5
4	OM	7840984	6.7	−12.9	0.2	2.8	14.6	0.3	11.2	0.6	0.5
4	OM	6180366	7.8	−11.8	0.2	2.8	15.3	0.4	11.3	0.7	0.5
4	OM	5999450	9.3	−10.3	0.2	2.8	15.7	0.3	10.9	0.3	0.5
4	OM	6047830	9.2	−10.4	0.4	2.8	15.6	0.4	10.8	0.3	0.5
4	OM	5723440	8.3	−11.3	0.3	2.8	14.9	0.3	10.6	0.1	0.5
4	MON	16173804	43.9	24.3	0.1	2.8	33.1	0.2	10.4	−0.2	0.5
4	MON	17073002	43.0	23.4	0.1	2.8	32.2	0.2	9.9	−0.7	0.5
4	MON	15223072	44.8	25.2	0.2	2.8	33.1	0.2	9.8	−0.7	0.5
5	Pyrite 1	19853441	7.6	−18.6	0.6	1.0	14.9	0.7	11.0	1.0	0.2
5	Pyrite 1	22141295	13.6	−12.5	0.8	1.0	16.6	0.7	9.6	−0.4	0.2
5	Pyrite 1	22665664	11.4	−14.7	0.8	1.0	16.6	0.7	10.6	0.7	0.2
5	Pyrite 2	17713296	15.7	−10.5	0.2	1.0	18.5	0.1	10.3	0.4	0.2
5	Pyrite 2	19756705	17.1	−9.1	0.2	1.0	18.9	0.2	10.0	0.1	0.2
5	Pyrite Std	15767140	36.7	10.5	0.2	1.0	28.9	0.2	9.9	0.0	0.2
5	Pyrite Std	15343253	35.7	9.6	0.2	1.0	28.7	0.2	10.2	0.3	0.2
5	Pyrite Std	14380903	34.0	7.9	0.2	1.0	27.4	0.2	9.8	−0.1	0.2
5	Pyrite 3	14633530	20.5	−5.6	0.2	1.0	20.5	0.2	9.9	0.0	0.2
5	Pyrite 3	14423422	20.8	−5.4	0.2	1.0	20.5	0.2	9.8	−0.2	0.2
5	Pyrite 3	13879523	19.8	−6.3	0.2	1.0	20.6	0.1	10.3	0.4	0.2
5	Pyrite Std	13826458	35.3	9.1	0.2	1.0	28.0	0.2	9.7	−0.3	0.2
5	Pyrite Std	13302279	34.8	8.6	0.1	1.0	27.9	0.2	9.9	0.0	0.2
5	Pyrite Std	12876311	34.4	8.2	0.1	1.0	28.0	0.2	10.1	0.2	0.2

*MON, kerogen isolated from Monterey Formation; GHA, kerogen from Ghareb Limestone; WIL, kerogen from the Wilcox group; OM, kerogen extracted from Strelley Pool stromatolite; Pyrite Std, pyrite standard with a $\delta^{34}S_{CDT}$ of 9‰; Pyrite x, pyrite crystals measured in situ from Strelley Pool stromatolite thin sections.

†^{32}S ion current expressed in counts per second.

‡Raw sulfur isotope composition of kerogen (i.e., noncorrected for instrumental mass fractionation) expressed in ‰ relative to the V-CDT standard.

§Sulfur isotope composition of kerogen corrected for instrumental mass fractionation and expressed in ‰ relative to the V-CDT standard.

¶Internal error (1σ).

‖Standard deviation (1σ) for the linear regression used to correct for the instrumental mass fractionation during each session.

**$\Delta^{33}S = \delta^{33}S_{CDT} − 0.5185 * \delta^{34}S_{CDT}$.

††Standard deviation (1σ) for the linear regression used to correct for the instrumental mass fractionation during each session. Bulk $\Delta^{33}S_{CDT}$ of MON, GHA, and WIL is unknown. The linear regression was made assuming that their average $\Delta^{33}S$ value equals 0.

Table S4. Data from NanoSIMS analyses

Session	Sample*	$^{34}S/^{32}S^{\dagger}$	^{32}S cps‡	$\delta^{34}S^{\S}$	$\sigma_{int}^{\P}$	$\Sigma_{IF}^{\parallel}$	K_{cor}^{**}	$\delta^{34}S^{\dagger\dagger}$	Si/C‡‡	O/C‡‡
1	Standard	0.0478	397502	27.1	0.5	0.7	0.0126	27.2		
1	Standard	0.0478	391503	27.5	0.5	0.7	0.0124	27.6		
1	Standard	0.0478	384792	27.7	0.5	0.7	0.0122	27.9		
1	Region 1	0.0468	5063	3.9	1.7	0.7	0.0002	7.4	0.12	1.51
1	Region 1	0.0468	7095	4.8	1.5	0.7	0.0002	8.2	0.13	1.14
1	Region 1	0.0472	5753	14.5	1.7	0.7	0.0002	18.0	0.08	1.29
1	Standard	0.0478	440279	28.0	0.5	0.7	0.0139	27.8		
1	Standard	0.0478	431134	27.1	0.5	0.7	0.0136	26.9		
1	Standard	0.0477	416411	25.9	0.5	0.7	0.0132	25.8		
2	Standard	0.0482	296053	28.6	0.6	1.7	0.0093	28.7		
2	Standard	0.0482	296942	28.4	0.6	1.7	0.0094	28.5		
2	Standard	0.0483	286103	29.1	0.6	1.7	0.0090	29.3		
2	Region 1	0.0470	5307	0.2	1.8	1.7	0.0002	2.8	0.16	2.36
2	Region 1	0.0469	7603	−2.2	1.5	1.7	0.0002	0.4	0.14	1.10
2	Region 1	0.0471	6144	2.1	1.7	1.7	0.0002	4.7	0.24	2.78
2	Standard	0.0481	332433	25.8	0.6	1.7	0.0105	25.6		
2	Standard	0.0481	321682	25.4	0.6	1.7	0.0102	25.3		
2	Standard	0.0481	325504	25.9	0.6	1.7	0.0103	25.8		
3	Standard	0.0479	373518	25.6	0.5	1.3	0.0118	25.8		
3	Standard	0.0480	404934	28.2	0.5	1.3	0.0128	28.2		
3	Standard	0.0480	397859	27.8	0.5	1.3	0.0126	27.8		
3	Standard	0.0480	388065	27.4	0.5	1.3	0.0123	27.5		
3	Standard	0.0479	380175	25.5	0.5	1.3	0.0120	25.7		
3	Region 2	0.0468	5707	1.2	1.7	1.3	0.0002	4.6	0.24	4.62
3	Region 2	0.0467	4485	−1.0	2.0	1.3	0.0001	2.4	0.34	8.43
3	Standard	0.0481	424201	29.3	0.4	1.3	0.0134	29.2		
3	Standard	0.0480	421809	26.8	0.5	1.3	0.0133	26.6		
3	Standard	0.0480	430738	27.1	0.4	1.3	0.0136	26.8		
4	Standard	0.0481	372664	28.3	0.6	1.7	0.0118	28.1		
4	Standard	0.0481	379485	26.8	0.6	1.7	0.0120	26.5		
4	Standard	0.0481	384121	28.7	0.6	1.7	0.0121	28.4		
4	Region 3	0.0472	2601	8.0	2.4	1.7	0.0001	10.9	0.55	7.50
4	Region 3	0.0483	2337	33.3	2.4	1.7	0.0001	36.2	0.78	7.33
4	Region 3	0.0480	892	24.9	4.2	1.7	0.0000	27.8	0.62	10.92
4	Standard	0.0482	367454	29.3	0.6	1.7	0.0116	29.1		
4	Standard	0.0482	372479	29.3	0.6	1.7	0.0118	29.1		
4	Standard	0.0481	371480	28.1	0.6	1.7	0.0117	27.9		
4	Region 2	0.0477	15533	17.9	1.5	1.7	0.0005	20.7	0.83	18.08
4	Region 2	0.0477	45115	19.2	0.9	1.7	0.0014	21.8	0.53	9.83
4	Region 2	0.0466	11003	−6.5	1.6	1.7	0.0003	−3.6	0.53	15.58
4	Region 2	0.0461	16473	−17.4	1.3	1.7	0.0005	−14.6	0.51	18.16
4	Region 2	0.0471	21560	6.4	1.1	1.7	0.0007	9.1	0.65	16.79
4	Standard	0.0481	344498	27.3	0.6	1.7	0.0109	27.3		
4	Standard	0.0481	346840	27.7	0.6	1.7	0.0110	27.7		
4	Standard	0.0480	345544	26.6	0.5	1.7	0.0109	26.5		
4	Standard	0.0480	280541	24.5	0.7	1.7	0.0089	25.0		
4	Standard	0.0479	284230	24.3	0.6	1.7	0.0090	24.9		
4	Standard	0.0480	288242	25.4	0.7	1.7	0.0091	25.9		
5	Standard	0.0483	401577	28.2	0.5	1.4	0.0127	28.0		
5	Standard	0.0483	402033	28.0	0.5	1.4	0.0127	27.8		
5	Standard	0.0483	397932	29.1	0.5	1.4	0.0126	29.0		
5	Region 4	0.0469	1753	−1.8	2.6	1.4	0.0001	1.5	0.01	3.34
5	Region 4	0.0470	2042	−1.1	2.3	1.4	0.0001	2.1	0.04	2.60
5	Standard	0.0482	364872	25.9	0.6	1.4	0.0115	26.1		
5	Standard	0.0482	361253	25.6	0.5	1.4	0.0114	25.8		
5	Standard	0.0482	360169	26.4	0.6	1.4	0.0114	26.6		
6	Standard	0.0486	322269	26.4	0.6	1.2	0.0149	25.9		
6	Standard	0.0486	300432	26.7	0.6	1.2	0.0138	26.5		
6	Region 5	0.0475	8273	1.7	2.6	1.2	0.0004	5.1	0.12	0.00
6	Region 5	0.0479	7890	10.1	2.6	1.2	0.0004	13.6	0.08	0.00
6	Region 5	0.0482	6550	18.2	3.0	1.2	0.0003	21.7	0.10	0.00
6	Standard	0.0487	275398	29.0	0.7	1.2	0.0127	29.1		
6	Standard	0.0486	243335	26.7	0.7	1.2	0.0112	27.2		
7	Standard	0.0486	293958	26.7	0.5	1.2	0.0135	27.1		
7	Standard	0.0486	312876	26.1	0.5	1.2	0.0144	26.3		
7	Standard	0.0486	320124	26.6	0.5	1.2	0.0148	26.7		
7	Standard	0.0487	363264	28.4	0.5	1.2	0.0168	27.9		
7	Region 5	0.0481	6536	14.1	2.5	1.2	0.0003	18.1	0.17	0.01
7	Region 5	0.0479	7259	9.3	2.0	1.2	0.0003	13.3	0.21	0.01

Session	Sample*	$^{34}S/^{32}S^†$	^{32}S cps‡	$\delta^{34}S^§$	$\sigma_{int}^¶$	$\Sigma_{IF}^‖$	K_{cor}**	$\delta^{34}S^{††}$	Si/C‡‡	O/C‡‡
7	Region 5	0.0485	7613	22.5	2.0	1.2	0.0003	26.5	0.16	0.01
7	Standard	0.0487	337484	27.5	0.5	1.2	0.0156	27.3		
7	Standard	0.0487	319235	26.9	0.5	1.2	0.0147	27.0		
7	Standard	0.0486	326966	26.7	0.5	1.2	0.0151	26.7		
7	Region 6	0.0472	4431	−5.7	2.7	1.2	0.0002	−1.7	0.27	0.01
7	Region 6	0.0471	4177	−7.9	2.5	1.2	0.0002	−3.9	0.13	0.01
7	Region 6	0.0470	3377	−10.0	2.5	1.2	0.0002	−6.0	0.23	0.01
7	Standard	0.0488	318134	30.1	0.5	1.2	0.0147	30.2		
7	Standard	0.0486	342831	25.7	0.5	1.2	0.0158	25.5		
7	Standard	0.0487	308832	27.0	0.6	1.2	0.0142	27.3		
7	Standard	0.0487	332213	27.3	0.5	1.2	0.0153	27.2		
8	Standard	0.0487	336473	28.1	0.5	0.7	0.0155	28.0		
8	Standard	0.0486	341332	27.1	0.6	0.7	0.0157	26.9		
8	Standard	0.0487	349612	27.8	0.5	0.7	0.0161	27.5		
8	Region 5	0.0491	3357	36.6	2.4	0.7	0.0002	40.6	0.27	0.02
8	Region 5	0.0481	2992	16.1	2.5	0.7	0.0001	20.2	0.25	0.02
8	Region 5	0.0478	4908	8.7	2.0	0.7	0.0002	12.7	0.13	0.01
8	Standard	0.0486	342644	25.7	0.5	0.7	0.0158	25.5		
8	Standard	0.0486	339981	26.9	0.5	0.7	0.0157	26.7		
8	Standard	0.0487	335867	27.5	0.5	0.7	0.0155	27.4		
8	Region 6	0.0473	1414	−2.3	4.1	0.7	0.0001	1.8	0.71	0.03
8	Region 6	0.0481	941	14.7	5.7	0.7	0.0000	18.8	0.91	0.09
8	Region 5	0.0477	7657	6.0	1.9	0.7	0.0004	10.0	0.10	0.00
8	Region 5	0.0478	8010	7.8	1.5	0.7	0.0004	11.9	0.12	0.00
8	Region 5	0.0478	4595	7.9	2.1	0.7	0.0002	11.9	0.11	0.00
8	Standard	0.0486	307018	26.8	0.5	0.7	0.0142	27.1		
8	Standard	0.0487	299312	27.9	0.6	0.7	0.0138	28.3		
8	Standard	0.0486	300101	27.1	0.5	0.7	0.0138	27.5		
9	Standard	0.0457	183497	26.3	0.7	1.5	0.0135	26.3		
9	Standard	0.0458	188289	27.6	0.7	1.5	0.0138	27.4		
9	Standard	0.0458	183769	28.9	0.8	1.5	0.0135	28.8		
9	Standard	0.0458	170046	28.4	0.8	1.5	0.0125	28.6		
9	Standard	0.0458	170012	28.0	0.8	1.5	0.0125	28.2		
9	Standard	0.0458	170597	28.3	0.8	1.5	0.0125	28.5		
9	Region 5	0.0446	2898	2.8	2.0	1.5	0.0002	6.1		
9	Region 5	0.0440	3736	−11.1	1.7	1.5	0.0003	−7.8		
9	Region 5	0.0444	3496	−2.9	1.8	1.5	0.0003	0.4		
9	Region 5	0.0436	2519	−19.9	2.1	1.5	0.0002	−16.6		
9	Region 5	0.0444	2959	−2.1	1.9	1.5	0.0002	1.2		
9	OM	0.0442	10356	−7.5	1.7	1.5	0.0008	−4.3		
9	Standard	0.0457	183482	25.3	0.8	1.5	0.0135	25.2		
9	Standard	0.0456	182760	24.8	0.8	1.5	0.0134	24.7		
10	Standard	0.0456	671077	27.3	0.5	1.1	0.0217	27.6		
10	Standard	0.0456	647321	27.5	0.5	1.1	0.0210	28.0		
10	Standard	0.0456	659001	27.8	0.4	1.1	0.0213	28.2		
10	OM	0.0433	7074	−22.2	1.8	1.1	0.0002	−16.4		
10	Standard	0.0456	840993	28.5	0.4	1.1	0.0273	27.3		
10	Standard	0.0456	844027	27.9	0.4	1.1	0.0274	26.8		
10	Standard	0.0456	853668	28.1	0.4	1.1	0.0277	26.9		
10	OM	0.0437	5651	−13.7	1.9	1.1	0.0002	−7.9		
10	Standard	0.0455	615024	26.1	0.5	1.1	0.0199	26.9		
10	Standard	0.0455	617301	26.3	0.5	1.1	0.0200	27.0		
10	Standard	0.0455	613173	25.3	0.5	1.1	0.0198	26.1		
11	Standard	0.0457	327403	27.1	0.6	1.9	0.0241	26.8		
11	Standard	0.0456	329220	26.5	0.6	1.9	0.0243	26.1		
11	Standard	0.0458	333370	30.7	0.6	1.9	0.0246	30.2		
11	Standard	0.0458	342374	30.8	0.6	1.9	0.0252	30.2		
11	Standard	0.0456	274765	25.3	0.6	1.9	0.0202	26.0		
11	Standard	0.0456	293003	25.6	0.6	1.9	0.0216	25.9		
11	Standard	0.0457	340654	27.9	0.6	1.9	0.0251	27.2		
11	Standard	0.0457	343648	28.0	0.6	1.9	0.0253	27.3		
11	OM	0.0438	14347	−15.4	1.4	1.9	0.0010	−9.8		
11	OM	0.0439	20147	−11.3	1.2	1.9	0.0015	−5.8		
11	OM	0.0439	28954	−13.0	1.0	1.9	0.0021	−7.7		
11	OM	0.0438	21238	−13.8	1.1	1.9	0.0015	−8.4		
11	OM	0.0445	28243	1.5	1.1	1.9	0.0021	6.8		
11	OM	0.0440	21716	−9.4	1.2	1.9	0.0016	−4.0		
11	Standard	0.0456	285293	26.4	0.6	1.9	0.0210	26.8		
11	Standard	0.0457	286855	26.7	0.6	1.9	0.0211	27.1		
11	Standard	0.0456	272591	26.0	0.7	1.9	0.0200	26.7		
11	Standard	0.0456	275771	25.4	0.7	1.9	0.0203	26.1		
12	Standard	0.0458	248382	27.1	0.7	1.8	0.0183	27.3		

Session	Sample*	$^{34}S/^{32}S^\dagger$	^{32}S cps‡	$\delta^{34}S^\S$	$\sigma_{int}^\P$	$\Sigma_{IF}^\|$	K_{cor}**	$\delta^{34}S^{\dagger\dagger}$	Si/C‡‡	O/C‡‡
12	Standard	0.0457	242779	26.2	0.7	1.8	0.0178	26.5		
12	Standard	0.0457	246996	25.7	0.7	1.8	0.0181	25.9		
12	Standard	0.0457	248168	26.0	0.7	1.8	0.0182	26.2		
12	Standard	0.0459	270288	30.0	0.6	1.8	0.0199	29.8		
12	Standard	0.0459	274166	30.3	0.6	1.8	0.0202	29.9		
12	OM	0.0442	9441	−8.1	1.7	1.8	0.0007	−3.4		
12	OM	0.0441	10664	−10.0	1.6	1.8	0.0008	−5.3		
12	OM	0.0443	10806	−5.3	1.6	1.8	0.0008	−0.7		
12	OM	0.0441	17024	−10.5	1.3	1.8	0.0012	−5.9		
12	OM	0.0438	8555	−16.0	1.9	1.8	0.0006	−11.3		
12	Standard	0.0457	261509	25.4	0.6	1.8	0.0192	25.3		
12	Standard	0.0457	260870	26.2	0.6	1.8	0.0192	26.2		
12	Standard	0.0458	263860	28.3	0.6	1.8	0.0194	28.2		
12	Standard	0.0458	267011	26.8	0.6	1.8	0.0196	26.7		
13	Standard	0.0457	193992	25.8	0.8	1.5	0.0142	27.1		
13	Standard	0.0457	187998	24.8	0.7	1.5	0.0138	26.3		
13	Standard	0.0458	231167	28.1	0.7	1.5	0.0170	28.7		
13	Standard	0.0458	239232	27.8	0.7	1.5	0.0176	28.2		
13	OM	0.0452	460850	13.2	0.3	1.5	0.0341	9.5		
13	OM	0.0456	587171	22.5	0.2	1.5	0.0437	16.3		
13	OM	0.0438	10412	−18.2	1.6	1.5	0.0008	−13.5		
13	OM	0.0439	11573	−15.2	1.6	1.5	0.0008	−10.5		
13	OM	0.0457	629673	24.7	0.2	1.5	0.0469	17.6		
13	Standard	0.0458	204420	26.9	0.7	1.5	0.0150	28.1		
13	Standard	0.0458	203117	28.3	0.8	1.5	0.0149	29.4		
13	Standard	0.0459	239531	29.1	0.7	1.5	0.0176	29.6		
13	Standard	0.0459	234018	29.3	0.7	1.5	0.0172	29.9		
14	Standard	0.0459	744371	29.2	0.4	1.9	0.0182	28.6		
14	Standard	0.0459	734279	29.1	0.4	1.5	0.0180	28.5		
14	Standard	0.0458	670243	26.5	0.4	1.5	0.0164	26.3		
14	Standard	0.0459	668646	27.9	0.4	1.5	0.0164	27.8		
14	Standard	0.0458	635653	26.2	0.4	1.5	0.0155	26.3		
14	Standard	0.0458	639004	25.7	0.4	1.5	0.0156	25.8		
14	Standard	0.0458	631126	27.1	0.4	1.5	0.0154	27.2		
14	Standard	0.0458	641810	25.8	0.4	1.5	0.0157	25.8		
14	SBB	0.0436	276573	−21.9	0.4	1.5	0.0067	−19.5		
14	SBB	0.0437	296009	−21.5	0.4	1.5	0.0072	−19.2		
14	SBB	0.0431	245317	−34.1	0.5	1.5	0.0060	−31.5		
14	SBB	0.0430	311988	−36.5	0.5	1.5	0.0076	−34.3		
14	SBB	0.0433	229615	−30.1	0.6	1.5	0.0056	−27.4		
14	SBB	0.0433	247002	−29.6	0.6	1.5	0.0060	−27.0		
14	SBB	0.0436	326854	−22.1	0.5	1.5	0.0080	−20.0		
14	SBB	0.0436	301872	−23.1	0.5	1.5	0.0074	−20.9		
14	SBB	0.0439	403861	−17.0	0.5	1.5	0.0099	−15.3		
14	SBB	0.0438	364072	−18.4	0.5	1.5	0.0089	−16.5		
14	SBB	0.0433	167487	−30.3	0.6	1.5	0.0041	−27.3		
14	SBB	0.0432	153104	−31.5	0.6	1.5	0.0037	−28.3		
14	SBB	0.0434	186001	−27.0	0.6	1.5	0.0045	−24.1		
14	SBB	0.0433	185739	−28.5	0.7	1.5	0.0045	−25.6		
14	Standard	0.0458	607838	26.3	0.4	1.5	0.0149	26.5		
14	Standard	0.0458	589074	26.0	0.5	1.5	0.0144	26.3		
14	GHA	0.0455	599595	19.1	0.8	1.5	0.0147	19.4		
14	GHA	0.0455	617689	20.6	0.5	1.5	0.0151	20.8		
14	GHA	0.0453	752195	14.6	0.4	1.5	0.0184	14.0		
14	GHA	0.0453	766552	15.3	0.8	1.5	0.0188	14.6		
14	GHA	0.0454	627992	16.3	0.4	1.5	0.0154	16.5		
14	GHA	0.0454	661269	17.5	0.4	1.5	0.0162	17.4		
14	GHA	0.0455	819873	19.0	0.4	1.5	0.0201	18.0		
14	GHA	0.0455	826526	19.9	0.4	1.5	0.0203	18.7		
14	GHA	0.0453	711850	15.4	0.4	1.5	0.0174	15.0		
14	GHA	0.0453	723731	15.8	0.4	1.5	0.0177	15.4		
14	GHA	0.0453	602270	15.5	0.5	1.5	0.0147	15.8		
14	GHA	0.0453	598057	15.8	0.5	1.5	0.0146	16.1		
14	GHA	0.0454	596846	17.2	0.5	1.5	0.0146	17.6		
14	GHA	0.0454	632604	17.4	0.4	1.5	0.0155	17.5		
14	WIL	0.0446	43503	0.3	1.1	1.5	0.0011	4.1		
14	WIL	0.0447	44051	1.1	1.1	1.5	0.0011	4.9		
14	WIL	0.0449	36904	6.2	1.2	1.5	0.0009	10.0		
14	WIL	0.0451	30187	9.7	1.4	1.5	0.0007	13.6		
14	WIL	0.0449	27694	6.2	1.4	1.5	0.0007	10.1		
14	WIL	0.0448	25006	5.2	1.5	1.5	0.0006	9.1		
14	WIL	0.0448	47893	3.5	1.1	1.5	0.0012	7.2		

Session	Sample*	$^{34}S/^{32}S^{\dagger}$	^{32}S cps‡	$\delta^{34}S^{\S}$	$\sigma_{int}^{\P}$	$\Sigma_{IF}^{\|}$	K_{cor}**	$\delta^{34}S^{\dagger\dagger}$	Si/C‡‡	O/C‡‡
14	WIL	0.0447	48944	2.7	1.1	1.5	0.0012	6.4		
14	WIL	0.0452	57327	12.1	1.0	1.5	0.0014	15.8		
14	WIL	0.0451	60850	10.5	0.9	1.5	0.0015	14.2		
14	WIL	0.0451	62556	10.7	0.9	1.5	0.0015	14.4		
14	Standard	0.0458	573859	25.4	0.5	1.5	0.0140	25.8		
14	Standard	0.0458	563333	26.0	0.5	1.5	0.0138	26.5		
14	Standard	0.0458	645058	27.2	0.4	1.5	0.0158	27.2		
14	Standard	0.0458	653409	27.0	0.5	1.5	0.0160	26.9		
14	Standard	0.0460	655143	29.7	0.4	1.5	0.0160	29.6		
14	Standard	0.0460	658777	30.1	0.5	1.5	0.0161	30.0		
15	Pyrite Std	0.0469	281560	9.6	0.9	1.0	0.0376	9.3		
15	Pyrite Std	0.047	281820	10.3	0.9	1.0	0.0376	10.0		
15	Pyrite Std	0.047	281579	10.4	0.9	1.0	0.0376	10.1		
15	Pyrite 1	0.0462	230784	−7.1	1.0	1.0	0.0308	−5.3		
15	Pyrite 1	0.0462	231057	−6.8	1.0	1.0	0.0308	−5.0		
15	Pyrite 1	0.0462	230275	−7.2	1.0	1.0	0.0307	−5.4		
15	Pyrite 2	0.0461	226551	−8.9	1.0	1.0	0.0302	−7.0		
15	Pyrite 2	0.0461	226027	−7.7	1.0	1.0	0.0302	−5.8		
15	Pyrite 2	0.0461	224265	−8.9	0.9	1.0	0.0299	−6.9		
15	Pyrite 3	0.0461	230217	−8.1	0.9	1.0	0.0307	−6.3		
15	Pyrite 3	0.0462	230151	−7.5	1.0	1.0	0.0307	−5.8		
15	Pyrite 3	0.0461	231956	−7.7	1.0	1.0	0.031	−6.0		
15	Pyrite Std	0.0469	277813	8.9	0.9	1.0	0.0371	8.8		
15	Pyrite Std	0.0469	278456	8.0	0.9	1.0	0.0372	7.9		
15	Pyrite Std	0.0469	279633	8.2	0.9	1.0	0.0373	8.0		

*Standard, kerogen isolated from Monterey Formation; Region x, in situ measurements from stromatolite thin sections; OM, kerogen extracted from Strelley Pool stromatolite; SBB, protokerogen from recent Santa Barbara Basin sediments; GHA, kerogen from Ghareb Limestone; WIL, kerogen from the Wilcox group; OD1, sulfide minerals from ore deposit; OD2, sulfide minerals from ore deposit; Pyrite Std, pyrite standard with a $\delta^{34}S_{CDT}$ of 9‰; Pyrite x, pyrite crystals measured in situ from Strelley Pool stromatolite thin sections.

†Raw isotope ratio corrected only for detector dead-time.

‡^{32}S ion current expressed in counts per second.

§Sulfur isotope composition of kerogen corrected for instrumental mass fractionation and expressed in ‰ relative to the V-CDT standard.

¶Internal error (1σ).

$^{\|}$Standard deviation (1σ) for the linear regression used to correct for the instrumental mass fractionation during each session.

**Corrected $^{32}S^{-}/Cs^{+}$ ratio used for QSA correction of $^{34}S/^{32}S$ ratios (see SOM).

††Sulfur isotope composition of kerogen corrected for instrumental mass fractionation and QSA, and expressed in ‰ relative to the V-CDT standard.

‡‡Elemental ratios are not corrected for instrumental mass fractionation. Thus, only data from the same session can be compared. During sessions 1 to 5, oxygen was measured as ^{16}O; from session 6 to 8, it was measured as ^{18}O.